LETTERS

Time-reversal symmetry breaking and spontaneous Hall effect without magnetic dipole order

Yo Machida[1]†, Satoru Nakatsuji[1], Shigeki Onoda[2], Takashi Tayama[1]† & Toshiro Sakakibara[1]

Spin liquids are magnetically frustrated systems, in which spins are prevented from ordering or freezing, owing to quantum or thermal fluctuations among degenerate states induced by the frustration. Chiral spin liquids are a hypothetical class of spin liquids in which the time-reversal symmetry is macroscopically broken in the absence of an applied magnetic field or any magnetic dipole long-range order. Even though such chiral spin-liquid states were proposed more than two decades ago[1–3], an experimental realization and observation of such states has remained a challenge. One of the characteristic order parameters in such systems is a macroscopic average of the scalar spin chirality, a solid angle subtended by three nearby spins. In previous experimental reports, however, the spin chirality was only parasitic to the non-coplanar spin structure associated with a magnetic dipole long-range order or induced by the applied magnetic field[4–10], and thus the chiral spin-liquid state has never been found. Here, we report empirical evidence that the time-reversal symmetry can be broken spontaneously on a macroscopic scale in the absence of magnetic dipole long-range order. In particular, we employ the anomalous Hall effect[4,11] to directly probe the broken time-reversal symmetry for the metallic frustrated magnet $Pr_2Ir_2O_7$. An onset of the Hall effect is observed at zero field in the absence of uniform magnetization, within the experimental accuracy, suggesting an emergence of a chiral spin liquid. The origin of this spontaneous Hall effect is ascribed to chiral spin textures[4,5,12,13], which are inferred from the magnetic measurements indicating the spin ice-rule formation[14,15].

The time-reversal symmetry (TRS) in equilibrium is one of the most fundamental symmetries in physics, and can be spontaneously broken by a phase transition in macroscopic systems. A typical example is a magnetic phase transition at which spin dipole moments form a long-range static configuration as in ferromagnets. Nevertheless, the source of the broken TRS is not restricted to conventional magnetic long-range order (LRO). Any product of an odd number of spins that is odd under the time-reversal, as is the spin itself, may become the primary yet hidden order parameter that breaks the TRS. The simplest but nontrivial product of this kind is the scalar spin chirality[1–3], which is the solid angle subtended by three neighbouring spins, $\kappa_{ijk} = \mathbf{S}_i \cdot \mathbf{S}_j \times \mathbf{S}_k$ (Fig. 1a). This raises an intriguing possibility of chiral spin liquids[3]. In this type of spin-liquid states, the TRS is broken spontaneously and macroscopically, for instance, by a LRO of scalar chirality, while the spin dipole moments are neither long-range-ordered nor frozen because of geometrical frustration of magnetic interaction. Despite intensive studies over decades, an experimental realization and observation of such chiral spin-liquid states remains a challenge.

A crucial step towards the observation is to find an appropriate experimental probe for this macroscopically broken TRS in the absence of magnetic dipole order. Neutron or X-ray scattering experiments can visualize a long-range magnetic structure when spins are essentially ordered. However, it is usually difficult to extract the scalar spin chirality κ_{ijk} reliably unless the spins are long-range-ordered[8]. In metallic magnets, on the other hand, a promising probe is available: the anomalous Hall effect (AHE)[4,11], which is the spontaneous Hall effect at zero applied magnetic field.

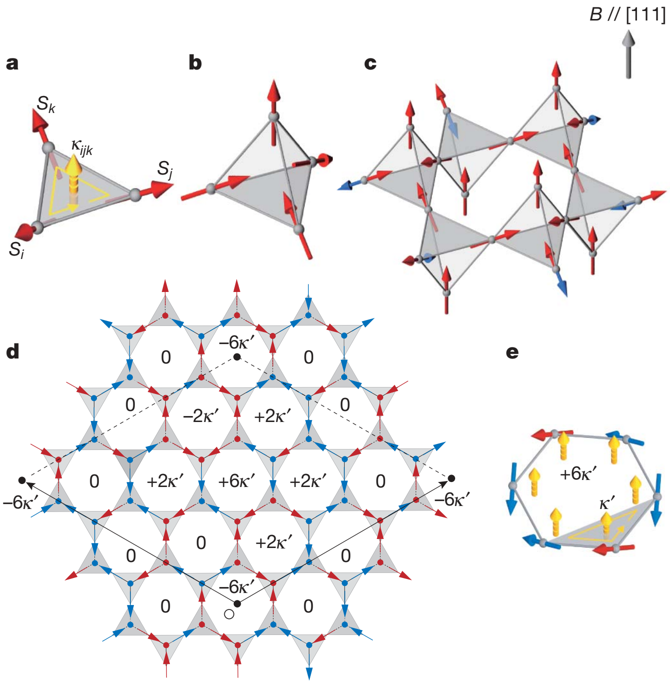

Figure 1 | Chiral spin state and pyrochlore lattice. **a**, Scalar spin chirality made of three non-coplanar spins on a triangle: $\kappa_{ijk} = \mathbf{S}_i \cdot \mathbf{S}_j \times \mathbf{S}_k$ (thick yellow arrow). The counterclockwise rotation (thin yellow arrow) indicates the order of spins in κ_{ijk}. **b**, '2-in, 2-out' configuration of four <111> Ising spins on a tetrahedron. **c**, Pyrochlore lattice formed by Pr^{3+} ions, which is an alternating stack of kagome (corner-sharing triangles) and triangular layers along the [111] direction. Under zero field, Pr 4*f* moments with an effective size of $p_{eff} \approx 2.7\mu_B$ per Pr atom most probably form the '2-in, 2-out' configuration as denoted by three red arrows and one blue arrow on each tetrahedron. Application of the field *B* along the [111] direction flips the moments shown as blue arrows and stabilizes the '3-in, 1-out' ('1-in, 3-out') configuration formed by four red arrows. **d**, Chiral antiferromagnetic spin configuration with zero magnetization as a possible snapshot in the TRS-broken phase ($T_f \leq T \leq T_H$) at zero field. The black arrows denote the translation vectors. Red and blue arrows indicate <111> Ising spins having a component parallel and another opposite to the field direction, respectively. **e**, Scalar spin chirality made of three neighbouring spins along a hexagon, κ', on a kagome layer and the sum, $6\kappa'$, over the edges. The sum for each hexagon is also shown for the chiral antiferromagnetic state in **d**, which has a nonvanishing uniform component in the antiferroic background.

[1]Institute for Solid State Physics, University of Tokyo, Kashiwa 277-8581, Japan. [2]Condensed Matter Theory Laboratory, RIKEN, Wako 351-0198, Japan. †Present addresses: Department of Physics, Tokyo Institute of Technology, Meguro 152-8551, Japan (Y.M.); Department of Physics, University of Toyama, Toyama 930-8555, Japan (T.T.).

Usually, the AHE arises in ferromagnets because the spontaneous magnetization breaks the TRS macroscopically even in the absence of applied magnetic field. The dominant part of the AHE in moderately dirty ferromagnetic metals can be captured by the band-intrinsic mechanism[4,16]. The adiabatic motion of electrons under an electric field $\boldsymbol{E}$ (ref. 17) acquires the Berry phase[18] because of the relativistic spin-orbit interaction and the net spin polarization. This phase acts as a macroscopic fictitious magnetic field $\boldsymbol{b}$ that bends the orbital motion of electrons like the Lorentz force does due to a real magnetic field $\boldsymbol{B}$. Thus, it causes the AHE characterized by a finite Hall conductivity σ_H at $B=0$.

In general, however, the source of the fictitious magnetic field $\boldsymbol{b}$, namely, the condition for observing the AHE at $B=0$, is not restricted to the magnetization, but to the macroscopically broken TRS[19], which means that the time-reversal operation cannot be compensated by any other symmetry operations of the crystal (Supplementary Information). In particular, the scalar spin chirality in non-coplanar ferromagnets or canonical spin glasses can also produce the fictitious field and thus the AHE[4,5,12,13,20], as indeed has been observed in $Nd_2Mo_2O_7$ (ref. 5), AuMn (refs 6, 7), and MnSi (refs 9, 10). In these pioneering works, however, the spin chirality is not the primary order parameter, but only accompanies a chiral spin texture of a magnetic dipole LRO or is induced by the applied magnetic field. Thus, it has remained an important open issue to find a possible chiral spin-liquid phase[3] by probing the macroscopically broken TRS through the AHE at zero magnetic field.

Here, we report the discovery of a TRS-broken phase in the absence of both magnetic dipole order and spin freezing in the thermodynamic measurements, suggesting a chiral spin-liquid state. In particular, we observed a spontaneous Hall effect in the absence of uniform magnetization within experimental accuracy in the metallic cooperative paramagnet $Pr_2Ir_2O_7$ above its spin freezing temperature, as indicated by the bifurcation of the susceptibility. Both the experiment and the theory suggest that a chiral spin-liquid phase is induced by melting of a spin ice, because the quantum fluctuations of the Pr 4*f* magnetic moments[21] were stronger than in dipolar spin-ice systems[14,15].

The pyrochlore iridate $Pr_2Ir_2O_7$ has an antiferromagnetic Curie–Weiss temperature $\Theta_W \approx -20$ K, mainly due to the correlations among $<111>$ 4*f* Ising magnetic moments of Pr^{3+} ions, which point either inwards to or outwards from the centre of the Pr tetrahedron (Fig. 1b and c)[22,23]. Ir 5*d* conduction electrons are weakly correlated and remain in a Pauli paramagnetic state[22]. They mediate the RKKY interaction between Pr 4*f* moments via the Kondo coupling. The absence of any sharp anomalies indicating conventional magnetic LRO in the measurements of specific heat, magnetic susceptibility, and muon spin relaxation (μSR)[22,24] signals strong geometrical frustration[15]. Only a spin freezing is observed in the magnetic susceptibility below $T_f \approx 0.3$ K, which is two orders of magnitude lower than $|\Theta_W| \approx 20$ K (ref. 22) (Fig. 2a). Therefore, below $|\Theta_W|$, the 4*f* moments probably remain in a cooperative paramagnetic state down to at least $T_f \approx 0.3$ K (refs 22, 24).

First, we show our main experimental evidence for the broken TRS found in the states where neither magnetic dipole LRO nor spin freezing is observed in thermodynamic measurements. Figure 2a presents the temperature dependence of the Hall conductivity $\sigma_H(T)$ (defined in the figure caption) measured at a low field of 0.05 T applied along the [111] direction. The zero-field-cooled and the field-cooled data of $\sigma_H(T)$ and thus the Hall resistivity $\rho_H(T)$ (Supplementary Fig. 1) bifurcate at $T_H \approx 1.5$ K, a temperature which is nearly an order of magnitude higher than $T_f \approx 0.3$ K, although the longitudinal conductivity $\sigma(T)$ (Fig. 2b, inset) and resistivity $\rho(T)$ (Supplementary Fig. 1) does not exhibit any detectable bifurcation. The bifurcation in $\sigma_H(T)$ suggests the emergence of a spontaneous component. To avoid a (partial) cancellation of σ_H due to a domain formation, we have performed field sweep measurements up to 7 T at various temperatures. Corresponding to the above bifurcation found in $\sigma_H(T)$, the field dependence of $\sigma_H(B)$ for $\boldsymbol{B}||[111]$ at $T < T_H \approx 1.5$ K shows a hysteresis between field up and down sweeps, which is accompanied by a finite

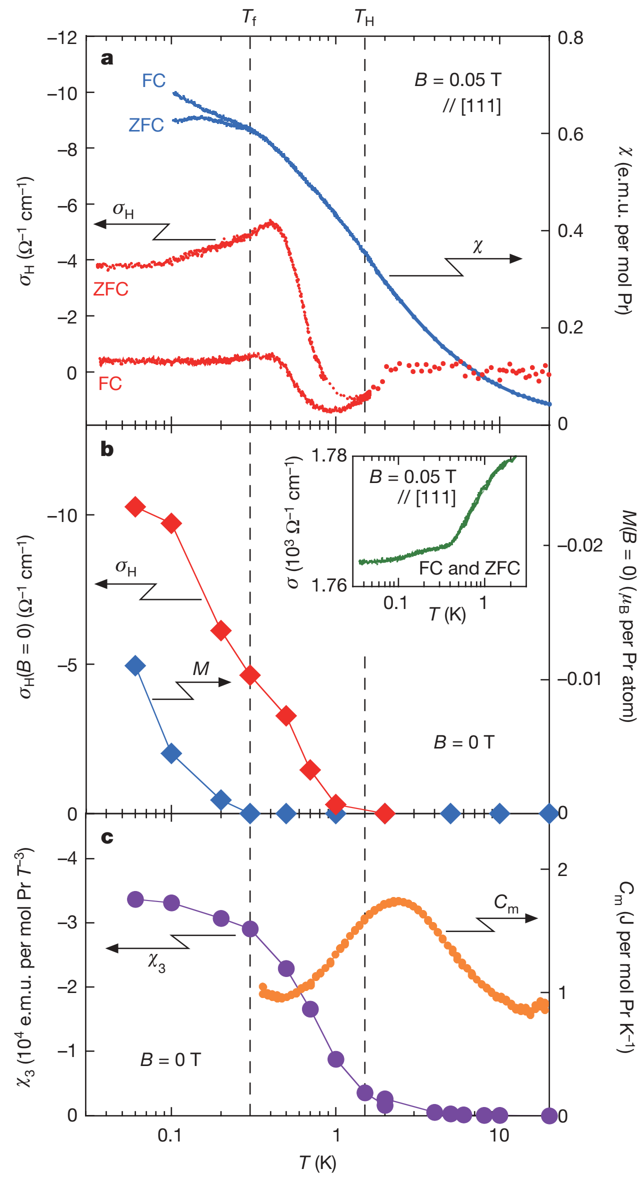

Figure 2 | Temperature dependence of the magnetic and transport properties of $Pr_2Ir_2O_2$. a, Temperature dependence of the Hall conductivity σ_H (left axis) and the direct-current susceptibility $\chi = M/H$ (right axis) under a magnetic field of $B = 0.05$ T along the [111] direction. e.m.u., electromagnetic unit. Here, Hall conductivity is given by $\sigma_H = -\rho_H/(\rho_H^2 + \rho^2)$, where ρ_H is the Hall resistivity and ρ is the longitudinal resistivity. Both the zero-field-cooled (ZFC) and field-cooled (FC) results are plotted. Vertical dashed lines denote $T_H \approx 1.5$ K and $T_f \approx 0.3$ K, respectively. **b**, Temperature dependence of the remnant Hall conductivity $\sigma_H(B=0)$ (left axis) and remnant magnetization $M(B=0)$ (right axis) at zero field, obtained after a field sweep down from 7 T in the hysteresis loop measurements (Supplementary Information). The inset shows the temperature dependence of the longitudinal conductivity $\sigma = 1/\rho$ under $B = 0.05$ T along the [111] direction. No hysteresis is found between the results obtained in the ZFC and FC sequences. **c**, Temperature dependence of the nonlinear susceptibility χ_3 (Supplementary Information) (left axis), and magnetic specific heat C_m (right axis) under zero field, adapted from ref. 22.

remnant Hall conductivity at $B=0$ (Fig. 3a, inset). In sharp contrast, the field dependence of the magnetization $M(B)$ shows no hysteresis within our experimental accuracy ($\sim 10^{-3} \mu_B$) at $T < T_H$, and only a small hysteresis at $T < T_f$ (Fig. 3b, inset). Our observations on $\sigma_H(B=0, T)$ and $M(B=0, T)$ at various temperatures are summarized in Fig. 2b. This is evidence of a remarkable separation between the two temperature scales T_H and T_f. Upon cooling, the TRS is broken spontaneously and macroscopically at T_H without any apparent LRO of

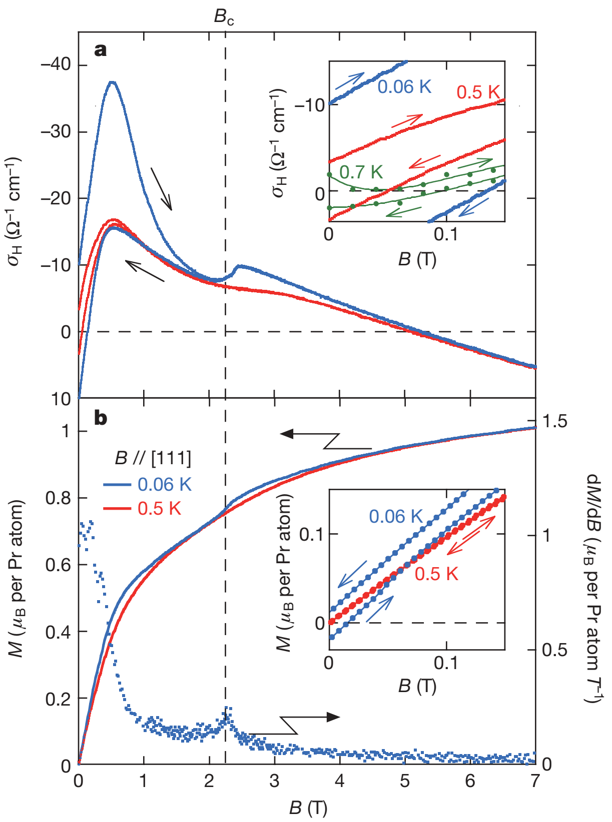

Figure 3 | Field dependence of the Hall conductivity and magnetization of $Pr_2Ir_2O_2$ along the [111] field direction. **a**, Field dependence of the Hall conductivity σ_H at 0.06 K and 0.5 K. **b**, Field dependence of the magnetization M at 0.06 K and 0.5 K (left axis) and its derivative dM/dB at 0.06 K (right axis). The dashed line represents the metamagnetic transition field $B_c \approx 2.3$ T. The inset to **a** shows low-field σ_H at fixed temperatures (0.06, 0.5 and 0.7 K). The green data points are taken at 0.7 K. The inset to **b** shows low-field M at fixed temperatures (0.06 and 0.5 K). The arrows in the insets and in panel **a** indicate up and down field sweep sequences. $\sigma_H(B)$ at 0.06 K (blue data points in **a**) shows a non-monotonous field dependence: first a pronounced hysteresis loop around $B = 0$ between the up-sweep $\sigma_H{}^{up}(B)$ and the down-sweep $\sigma_H{}^{down}(B)$, then a peak formation at $B_p \approx 0.5$ T, then a kink due to the metamagnetic transition at $B = B_c \approx 2.3$ T, and finally a sign change around 5 T. The remnant Hall conductivity $\sigma_H(B = 0)$ amounts to $10\,\Omega^{-1}\,cm^{-1}$, which is comparable to that for the ferromagnet $Nd_2Mo_2O_7$ (ref. 5). The size of the hysteresis, that is, $\sigma_H{}^{up}(B) - \sigma_H{}^{down}(B)$, decreases with field and vanishes at $B \approx B_c$, indicating that the '2-in, 2-out' state causes the hysteresis.

magnetic dipole moments, which is followed by spin freezing at a lower temperature T_f found in $\chi(T)$. This probably indicates the emergence of a TRS-broken spin-liquid phase caused by LRO or freezing of higher-order degrees of freedom than spin-dipole moments, for instance, the spin chirality.

We have also found solid evidence for the '2-in, 2-out' magnetic correlations (Fig. 1b) of Pr $4f$ <111> moments, which can be induced by a ferromagnetic interaction between them. Figure 3b shows the magnetization $M(B)$ for fields applied along the [111] direction. In contrast with $M(B)$ at 0.5 K, a small step feature is found at 0.06 K. This anomaly is more clearly observed as a kink in the derivative with respect to the field (Fig. 3b). At a lower temperature of 0.03 K, a hysteretic step is seen in $M(B)$, indicating a first-order metamagnetic transition (Supplementary Fig. 2, inset). In contrast, magnetization curves for fields along the [100] and [110] directions show neither an anomaly nor a hysteresis, just a smooth increase with field (Supplementary Fig. 2). The metamagnetism found only for the [111] direction indicates a ferromagnetic coupling between the nearest-neighbour Pr moments, and thus the transition between the low-field '2-in, 2-out' state and the high-field '3-in, 1-out' state (Fig. 1c), as observed in dipolar spin-ice systems[25].

Here, an analogy with dipolar spin-ice systems is very useful. For the spin ice, the magnetization M_c just below the metamagnetic transition field B_c and the effective nearest-neighbour ferromagnetic coupling J_{ff}^{eff} can be estimated using effective moment size p_{eff} and B_c (Supplementary Information)[14,25]. Our estimate of $M_c = 0.9\mu_B$ per Pr atom is close to the observed value $M_c \approx 0.8\mu_B$ per Pr atom (Fig. 3b). In addition, J_{ff}^{eff} is found to be about -1.4 K for $Pr_2Ir_2O_7$, which is close to the temperature (~2 K) where a peak is seen in the magnetic specific heat C_m as in spin-ice systems[14] (Fig. 2c). Around this temperature, the nonlinear magnetic susceptibility χ_3 also exhibits a steep negative increase, and saturates to a large negative value at lower temperatures. This is also consistent with ferromagnetic correlations due to $J_{ff}^{eff} \approx -1.4$ K (ref. 26) (Fig. 2c). Therefore, we conclude that the '2-in, 2-out' configurations have the largest amplitude in the state at $T \leq |J_{ff}^{eff}|$. On the other hand, there exist striking differences from dipolar spin-ice systems. The Curie–Weiss temperature Θ_W is not ferromagnetic as in $Dy_2Ti_2O_7$ (ref. 14), but antiferromagnetic as in $Tb_2Ti_2O_7$ (ref. 27), suggesting the quantum melting of spin ice[21,28] or contributions of more-distant-neighbour couplings[29]. In addition, the magnetic dipole interaction is an order of magnitude smaller for Pr^{3+} (~0.1 K) than for Dy^{3+} (~1 K) of the dipolar spin-ice system $Dy_2Ti_2O_7$ (ref. 14), and hence it can be even smaller than the f–f exchange interaction, which can be ferromagnetic and contain nontrivial quantum aspects[21].

Now, we mention a close relationship between the macroscopic TRS-breaking and the local '2-in, 2-out' spin correlations. The onset temperature $T_H \approx 1.5$ K almost coincides with the effective ferromagnetic coupling $|J_{ff}^{eff}| \approx 1.4$ K. Furthermore, the hysteresis observed in σ_H as a function of field disappears at the metamagnetic critical field B_c at which a sizeable fraction of the '2-in, 2-out' configurations are transformed into the '3-in, 1-out' configuration (Fig. 3a and b). Therefore, it is natural to expect that the macroscopically TRS-broken state found for $T_f \leq T \leq T_H$ consists of '2-in, 2-out' configurations for each tetrahedron and simultaneously has a non-zero macroscopic average of some sort of spin chirality.

Although the '2-in, 2-out' state made of four Ising spins locally possesses a scalar chirality, it is not trivial to determine whether a macroscopic chiral state with a zero net Pr moment can be constructed using these local '2-in, 2-out' units. Here, we show that it is indeed possible by giving a specific example in Fig. 1d. In this configuration, the spatial average of the chirality defined on each triangle (Fig. 1a) vanishes. However, the chirality κ' along the hexagon (Fig. 1e) produces a nonvanishing uniform component in an antiferroic background, suggesting a macroscopically broken TRS. Similar chiral spin configurations having the same uniform chirality $\langle\kappa'\rangle$ can also be obtained by $\pm 120°$ rotations (for example, about the origin O in Fig. 1d) and/or by translation. There are even more complicated long-period structures having the same sign of $\langle\kappa'\rangle$. We note that the ordered spin-ice state[14,30] can be ruled out, because it does not break the TRS macroscopically and so it does not produce the AHE at zero magnetic field.

Next, we demonstrate that a chiral spin configuration such as is shown in Fig. 1d actually gives rise to a finite anomalous Hall conductivity σ_H. We take a tight-binding model for the t_{2g} manifold associated with Ir $5d$ conduction electrons that are subject to an appreciable spin-orbit coupling and an antiferromagnetic Kondo coupling to Pr $4f$ Ising moments (Supplementary Information). The intrinsic anomalous Hall conductivity[4,16,17] around the [111] axis, $\sigma_H = (\sigma_{xy} + \sigma_{yz} + \sigma_{zx})/\sqrt{3}$, is obtained through, for instance:

$$\sigma_{xy} = -\frac{e^2}{\hbar}\int\frac{d\mathbf{k}}{(2\pi)^3}\sum_n f(\varepsilon_{n\mathbf{k}})b^z_{n\mathbf{k}} \qquad (1)$$

with $-e$ the electronic charge, $\varepsilon_{n\mathbf{k}}$ the band dispersion, and f the Fermi distribution function. Here, the Berry-phase curvature is obtained as:

$$\mathbf{b}_{n\mathbf{k}} = \nabla_{\mathbf{k}} \times \mathbf{a}_{n\mathbf{k}} \qquad (2)$$

from the Berry-phase connection $\mathbf{a}_{n\mathbf{k}} = i\langle u_{n\mathbf{k}}|\nabla_{\mathbf{k}}|u_{n\mathbf{k}}\rangle$ for the Bloch wavefunction $|u_{n\mathbf{k}}\rangle$ At zero field, the theory gives a small but finite value $\sigma_H = 0.2\,\Omega^{-1}\,\mathrm{cm}^{-1}$, in qualitative agreement with the experiment. However, the experimental value of the nontrivial AHE in the TRS-broken phase steeply increases below T_H to a much larger value than this simple band-intrinsic result. This enhancement of σ_H may be attributed to ferromagnetic fluctuations, which were not taken into account in the above calculation.

We note that the Berry-phase curvature $\boldsymbol{b}_{n\mathbf{k}}$ also produces a uniform orbital magnetization density owing to the circulating orbital motion of conduction electrons. However, given the present experimental results showing zero total magnetization, this orbital magnetic moment could be too small to detect or could be cancelled by the contribution from the spins. Indeed, for the configuration shown in Fig. 1d, both the orbital and the spin magnetic moments are calculated as $\sim 10^{-6}\mu_B$ per $PrIrO_{3.5}$ unit (Supplementary Information) which are much smaller than the present experimental accuracy for magnetization measurements.

In fact, the absence of both magnetic dipole LRO and spin freezing above T_f in the thermodynamic and μSR measurements suggests that spin-ice states with a uniform chirality component such as the one shown in Fig. 1d should become dynamic at $T \gtrsim T_f$ in $Pr_2Ir_2O_7$, forming a three-dimensional chiral spin-liquid state. In this system, quantum fluctuations should be enhanced compared with dipolar spin-ice systems, reflecting the small moment size, and may give rise to quantum entangled spin-ice states[21,28]. The above configuration, having a uniform component of the chirality κ', yields a finite σ_H through the Kondo coupling to the Ir $5d$ conduction electrons, so all the symmetry-related states with the same chirality have the same σ_H. Even though some other chiral '2-in, 2-out' configurations should be superimposed to form the chiral spin liquid, σ_H does not vanish as long as this spin liquid state has a uniform chirality.

Important issues to be clarified are the spatial and dynamical profiles of the spin and the chirality. In a chiral spin-liquid state, the chirality may form either a LRO or a frozen state to break the TRS in a macroscopic scale below T_H. This could involve a small internal field created by the chiral spin texture and/or the orbital motion of itinerant electrons, though it has not been detected in the susceptibility and μSR measurements down to T_f. The experimental determination of the magnetic and chirality correlations in the TRS-broken phase for $T_f \lesssim T \lesssim T_H$ is left for future studies.

Received 18 May; accepted 18 November 2009.
Published online 9 December 2009.

1. Baskaran, G. & Anderson, P. W. Gauge theory of high-temperature superconductors and strongly correlated Fermi systems. *Phys. Rev. B* **37**, 580–583 (1988).
2. Laughlin, R. B. The relationship between high-temperature superconductivity and the fractional quantum Hall effect. *Science* **242**, 525–533 (1988).
3. Wen, X. G., Wilczek, F. & Zee, A. Chiral spin states and superconductivity. *Phys. Rev. B* **39**, 11413–11423 (1989).
4. Nagaosa, N., Sinova, J., Onoda, S., MacDonald, A. & Ong, N. P. Anomalous Hall effect. Preprint at ⟨http://arxiv.org/abs/0904.4154⟩ (2009).
5. Taguchi, Y., Oohara, Y., Yoshizawa, H., Nagaosa, N. & Tokura, Y. Spin chirality, Berry phase, and anomalous Hall effect in a frustrated ferromagnet. *Science* **291**, 2573–2576 (2001).
6. Taniguchi, T. *et al.* Direct observation of chiral susceptibility in the canonical spin glass AuFe. *Phys. Rev. Lett.* **93**, 246605 (2004).
7. Pureur, P., Fabris, F. W., Schaf, J. & Campbell, I. A. Chiral susceptibility in canonical spin glass and reentrant alloys from Hall effect measurements. *Europhys. Lett.* **67**, 123–129 (2004).
8. Grohol, D. *et al.* Spin chirality on a two-dimensional frustrated lattice. *Nature Mater.* **4**, 323–328 (2005).
9. Neubauer, A. *et al.* Topological Hall effect in the A phase of MnSi. *Phys. Rev. Lett.* **102**, 186602 (2009).
10. Lee, M., Kang, W., Onose, Y., Tokura, Y. & Ong, N. P. Unusual Hall effect anomaly in MnSi under pressure. *Phys. Rev. Lett.* **102**, 186601 (2009).
11. Hall, E. H. On the 'rotational coefficient' in nickel and cobalt. *Proc. Phys. Soc. Lond.* **4**, 325–342 (1880).
12. Ye, J. *et al.* Berry phase theory of the anomalous Hall effect: application to colossal magnetoresistance manganites. *Phys. Rev. Lett.* **83**, 3737–3740 (1999).
13. Kawamura, H. Anomalous Hall effect as a probe of the chiral order in spin glasses. *Phys. Rev. Lett.* **90**, 047202 (2003).
14. Bramwell, S. T. & Gingras, M. J. P. Spin ice state in frustrated magnetic pyrochlore materials. *Science* **294**, 1495–1501 (2001).
15. Moessner, R. & Ramirez, A. Geometrical frustration. *Phys. Today* **59**, 24–29 (2006).
16. Thouless, D. J., Kohmoto, M., Nightingale, M. P. & den Nijs, M. Quantized Hall conductance in a two-dimensional periodic potential. *Phys. Rev. Lett.* **49**, 405–408 (1982).
17. Sundaram, G. & Niu, Q. Wave-packet dynamics in slowly perturbed crystals: gradient corrections and Berry-phase effects. *Phys. Rev. B* **59**, 14915–14925 (1999).
18. Berry, M. V. Quantum phase factors accompanying adiabatic changes. *Proc. R. Soc. Lond. A* **392**, 45–57 (1984).
19. Landau, L. D. & Lifshitz, E. M. *Electrodynamics of Continuous Media* 2nd edn (Elsevier, 1984).
20. Metalidis, G. & Bruno, P. Topological Hall effect studied in simple models. *Phys. Rev. B* **74**, 045327 (2006).
21. Onoda, S. & Tanaka, Y. Quantum melting of spin ice into spin smectic with cooperative quadrupole and chirality. Preprint at ⟨http://arxiv.org/abs/0907.2536⟩ (2009).
22. Nakatsuji, S. *et al.* Metallic spin-liquid behavior of the geometrically frustrated Kondo lattice $Pr_2Ir_2O_7$. *Phys. Rev. Lett.* **96**, 087204 (2006).
23. Machida, Y. *et al.* Unconventional anomalous Hall effect enhanced by a noncoplanar spin texture in the frustrated Kondo lattice $Pr_2Ir_2O_7$. *Phys. Rev. Lett.* **98**, 057203 (2007).
24. MacLaughlin, D. E. *et al.* Weak quasistatic magnetism in the frustrated Kondo lattice $Pr_2Ir_2O_7$. *Physica B* **404**, 667–670 (2009).
25. Sakakibara, T., Tayama, T., Hiroi, Z., Matsuhira, K. & Takagi, S. Observation of a liquid-gas type transition in the pyrochlore spin ice compound $Dy_2Ti_2O_7$ in a magnetic field. *Phys. Rev. Lett.* **90**, 207205 (2003).
26. Wada, K. & Takayama, H. Nonlinear susceptibilities of the Sherrington-Kirkpatrick model and the spherical model. *Prog. Theor. Phys.* **64**, 327–329 (1980).
27. Gardner, J. S. *et al.* Cooperative paramagnetism in the geometrically frustrated pyrochlore antiferromagnet $Tb_2Ti_2O_7$. *Phys. Rev. Lett.* **82**, 1012–1015 (1999).
28. Molavian, H. R., Gingras, M. J. & Canals, B. Dynamically induced frustration as a route to a quantum spin ice state in $Tb_2Ti_2O_7$ via virtual crystal field excitations and quantum many body effects. *Phys. Rev. Lett.* **98**, 157204 (2007).
29. Ikeda, A. & Kawamura, H. Ordering of the pyrochlore Ising model with the long-range RKKY interaction. *J. Phys. Soc. Jpn* **77**, 073707 (2008).
30. Siddharthan, R., Shastry, B. S. & Ramirez, A. P. Spin ordering and partial ordering in holmium titanate and related systems. *Phys. Rev. B* **63**, 184412 (2001).

Supplementary Information is linked to the online version of the paper at www.nature.com/nature.

Acknowledgements We thank L. Balicas, H. Kawamura, Y. Maeno, Y. Matsumoto, N. Nagaosa, Y. Ohta and T. Taniguchi for their support and discussions. This work is partially supported by Grants-in-Aid from the Japanese Society for the Promotion of Science, by Grants-in-Aid for Scientific Research on Priority Areas and Scientific Research on Innovative Areas from the Ministry of Education, Culture, Sports, Science and Technology, Japan, and by the Kurata Grant. Y.M. is supported by JSPS research fellowships. The calculations were performed in part by using the RIKEN Super Combined Cluster (RSCC).

Author Contributions S.N. planned the experimental project, and Y.M. and S.N. collected data and wrote the paper; S.O. gave the theoretical interpretation, performed the calculations, and wrote the paper; T.T. and T.S. collected data. All authors discussed the results and commented on the manuscript.

Author Information Reprints and permissions information is available at www.nature.com/reprints. The authors declare no competing financial interests. Correspondence and requests for materials should be addressed to S.N. (satoru@issp.u-tokyo.ac.jp).